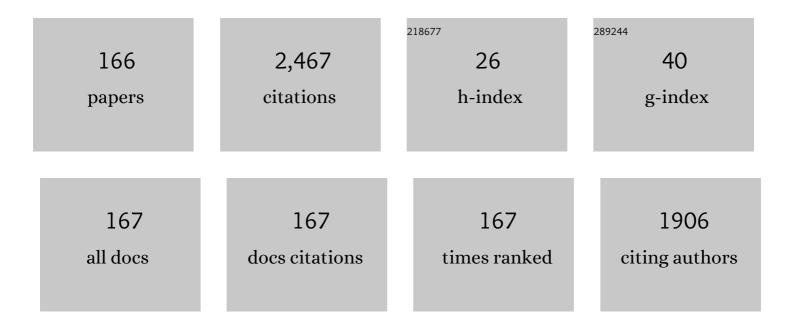
Tetsuo Uchikoshi

List of Publications by Year in descending order

Source: https://exaly.com/author-pdf/9023109/publications.pdf Version: 2024-02-01



#	Article	IF	CITATIONS
1	Effect of polyethylenimine on the dispersion and electrophoretic deposition of nano-sized titania aqueous suspensions. Journal of the European Ceramic Society, 2006, 26, 1555-1560.	5.7	124
2	Control of texture in alumina by colloidal processing in a strong magnetic field. Science and Technology of Advanced Materials, 2006, 7, 356-364.	6.1	106
3	Dense, bubble-free ceramic deposits from aqueous suspensions by electrophoretic deposition. Journal of Materials Research, 2001, 16, 321-324.	2.6	91
4	Electrophoretic Deposition Behavior of Aqueous Nanosized Zinc Oxide Suspensions. Journal of the American Ceramic Society, 2002, 85, 2161-2165.	3.8	74
5	Experimental verification of pH localization mechanism of particle consolidation at the electrode/solution interface and its application to pulsed DC electrophoretic deposition (EPD). Journal of the European Ceramic Society, 2010, 30, 1187-1193.	5.7	70
6	Bubbleâ€Free Aqueous Electrophoretic Deposition (EPD) by Pulseâ€Potential Application. Journal of the American Ceramic Society, 2008, 91, 3154-3159.	3.8	68
7	Reduced thermal degradation of the red-emitting Sr ₂ Si ₅ N ₈ :Eu ²⁺ phosphor via thermal treatment in nitrogen. Journal of Materials Chemistry C, 2015, 3, 7642-7651.	5.5	60
8	Electrophoretic deposition of alumina suspension in a strong magnetic field. Journal of the European Ceramic Society, 2004, 24, 225-229.	5.7	55
9	Fabrication and some properties of textured alumina-related compounds by colloidal processing in high-magnetic field and sintering. Journal of the European Ceramic Society, 2008, 28, 935-942.	5.7	55
10	Fabrication of porous ceramics with controlled pore size by colloidal processing. Science and Technology of Advanced Materials, 2005, 6, 915-920.	6.1	49
11	Control of crystalline texture in polycrystalline TiO2 (Anatase) by electrophoretic deposition in a strong magnetic field. Journal of the European Ceramic Society, 2006, 26, 559-563.	5.7	49
12	Electrophoretic deposition of aqueous nano-sized zinc oxide suspensions on a zinc electrode. Materials Research Bulletin, 2003, 38, 207-212.	5.2	46
13	Effect of Polyethylenimine on Hydrolysis and Dispersion Properties of Aqueous Si3N4Suspensions. Journal of the American Ceramic Society, 2007, 90, 797-804.	3.8	46
14	Tri-axial Grain Orientation of Y ₂ Ba ₄ Cu ₇ O _{<i>y</i>} Achieved by the Magneto-science Method. Applied Physics Express, 0, 1, 111701.	2.4	46
15	New ultra-violet and near-infrared blocking filters for energy saving applications: fabrication of tantalum metal atom cluster-based nanocomposite thin films by electrophoretic deposition. Journal of Materials Chemistry C, 2017, 5, 10477-10484.	5.5	41
16	Texture Development in Si3N4 Ceramics by Magnetic Field Alignment during Slip Casting. Journal of the Ceramic Society of Japan, 2006, 114, 979-987.	1.3	40
17	Electrophoretic deposition of lead zirconate titanate (PZT) powder from ethanol suspension prepared with phosphate ester. Science and Technology of Advanced Materials, 2005, 6, 927-932.	6.1	37
18	Mo ₆ cluster-based compounds for energy conversion applications: comparative study of photoluminescence and cathodoluminescence. Science and Technology of Advanced Materials, 2017, 18, 458-466.	6.1	37

#	Article	IF	CITATIONS
19	Prevention of thermal- and moisture-induced degradation of the photoluminescence properties of the Sr ₂ Si ₅ N ₈ :Eu ²⁺ red phosphor by thermal post-treatment in N ₂ –H ₂ . Physical Chemistry Chemical Physics, 2016, 18, 12494-12504.	2.8	36
20	Magnetic orientation and magnetic anisotropy in paramagnetic layered oxides containing rare-earth ions. Science and Technology of Advanced Materials, 2009, 10, 014604.	6.1	35
21	Inorganic Molybdenum Clusters as Lightâ€Harvester in All Inorganic Solar Cells: A Proof of Concept. ChemistrySelect, 2016, 1, 2284-2289.	1.5	35
22	Forming and Microstructure Control of Ceramics by Electrophoretic Deposition (EPD). KONA Powder and Particle Journal, 2010, 28, 74-90.	1.7	31
23	Mechanical properties of textured, multilayered alumina produced using electrophoretic deposition in a strong magnetic field. Journal of the European Ceramic Society, 2006, 26, 661-665.	5.7	30
24	Fabrication of multilayered oxide thermoelectric modules by electrophoretic deposition under high magnetic fields. Applied Physics Letters, 2006, 89, 081912.	3.3	30
25	Electrophoretic deposition of α-alumina particles in a strong magnetic field. Journal of Materials Research, 2003, 18, 254-256.	2.6	29
26	Surface modification of Ca-α-SiAlON: Eu2+ phosphor particles by SiO2 coating and fabrication of its deposit by electrophoretic deposition (EPD) process. Applied Surface Science, 2013, 280, 229-234.	6.1	28
27	Electrophoretic Deposition of <scp><scp>Ti</scp></scp> ₃ <scp><scp>SiC</scp>₂ and Texture Development in a Strong Magnetic Field. Journal of the American Ceramic Society, 2012, 95, 2857-2862.</scp>	3.8	27
28	Conductive Polymer Coating on Nonconductive Ceramic Substrates for Use in the Electrophoretic Deposition Process. Journal of the American Ceramic Society, 2008, 91, 1674-1677.	3.8	26
29	Extended Study on Electrophoretic Deposition Process of Inorganic Octahedral Metal Clusters: Advanced Multifunctional Transparent Nanocomposite Thin Films. Bulletin of the Chemical Society of Japan, 2018, 91, 1763-1774.	3.2	26
30	Preparation of Crystallineâ€Oriented Titania Photoelectrodes on ITO Glasses from a 2â€Propanol–2,4â€Pentanedione Solvent by Electrophoretic Deposition in a Strong Magnetic Field. Journal of the American Ceramic Society, 2009, 92, 984-989.	3.8	25
31	Visible tunable lighting system based on polymer composites embedding ZnO and metallic clusters: from colloids to thin films. Science and Technology of Advanced Materials, 2016, 17, 443-453.	6.1	25
32	pH localization: a case study during electrophoretic deposition of ternary MAX phase carbide-Ti ₃ SiC ₂ . Journal of the Ceramic Society of Japan, 2013, 121, 348-354.	1.1	23
33	Electrophoretically Deposited Layers of Octahedral Molybdenum Cluster Complexes: A Promising Coating for Mitigation of Pathogenic Bacterial Biofilms under Blue Light. ACS Applied Materials & Interfaces, 2020, 12, 52492-52499.	8.0	23
34	Texture Development in Alumina Composites by Slip Casting in a Strong Magnetic Field. Journal of the Ceramic Society of Japan, 2006, 114, 59-62.	1.3	22
35	Stabilization of Yttria Aqueous Suspension with Polyethylenimine and Electrophoretic Deposition Journal of the Ceramic Society of Japan, 2002, 110, 840-843.	1.3	21
36	Fabrication of Textured α-SiC Using Colloidal Processing and a Strong Magnetic Field. Materials Transactions, 2007, 48, 2883-2887.	1.2	20

#	Article	IF	CITATIONS
37	Phosphate Esters as Dispersants for the Cathodic Electrophoretic Deposition of Alumina Suspensions. Journal of the American Ceramic Society, 2008, 91, 1923-1926.	3.8	20
38	Fabrication of GDC/LSGM/GDC tri-layers on polypyrrole-coated NiO-YSZ by electrophoretic deposition for anode-supported SOFC. Journal of the Ceramic Society of Japan, 2009, 117, 1246-1248.	1.1	20
39	Emission color tuning of laminated and mixed SiAlON phosphor films by electrophoretic deposition. Journal of the Ceramic Society of Japan, 2010, 118, 1-4.	1.1	20
40	Ideal design of textured LiCoO2 sintered electrode for Li-ion secondary battery. APL Materials, 2013, 1, .	5.1	20
41	Electrophoretic Deposition of Alumina on Conductive Polymer-Coated Ceramic Substrates. Journal of the Ceramic Society of Japan, 2006, 114, 55-58.	1.3	19
42	Enhanced piezoelectric properties of grain-oriented Bi4Ti3O12–BaBi4Ti4O15 ceramics obtained by magnetic-field-assisted electrophoretic deposition method. Journal of Applied Physics, 2008, 104, .	2.5	19
43	Electrophoretic fabrication of a-b plane oriented La2NiO4 cathode onto electrolyte in strong magnetic field for low-temperature operating solid oxide fuel cell. Journal of the European Ceramic Society, 2016, 36, 4077-4082.	5.7	19
44	Evidence of the Ambipolar Behavior of Mo ₆ Cluster Iodides in All-Inorganic Solar Cells: A New Example of Nanoarchitectonic Concept. ACS Applied Materials & Interfaces, 2022, 14, 1347-1354.	8.0	19
45	Alignment of TiO2 particles by electrophoretic deposition in a high magnetic field. Materials Research Bulletin, 2004, 39, 2155-2161.	5.2	17
46	High-concentration niobium (V) doping into TiO ₂ nanoparticles synthesized by thermal plasma processing. Journal of Materials Research, 2011, 26, 658-671.	2.6	17
47	Zn-Al layered double hydroxide-based nanocomposite functionalized with an octahedral molybdenum cluster exhibiting prominent photoactive and oxidation properties. Applied Clay Science, 2020, 196, 105765.	5.2	16
48	Fabrication of porous (Ba,Sr)(Co,Fe)O3-δ (BSCF) ceramics using gelatinization and retrogradation phenomena of starch as pore-forming agent. Ceramics International, 2020, 46, 13047-13053.	4.8	16
49	Dispersion of SiC Suspensions with Cationic Dispersant of Polyethylenimine. Journal of the Ceramic Society of Japan, 2005, 113, 584-587.	1.3	15
50	Highly Texturing \hat{l}^2 -Sialon Via Strong Magnetic Field Alignment. Journal of the American Ceramic Society, 2008, 91, 620-623.	3.8	15
51	Twoâ€Dimensional Orientation in <scp><scp>Bi</scp></scp> ₄ <scp><fi< scp="">3<scp>O</scp> Prepared Using Platelet Particles and a Magnetic Field. Journal of the American Ceramic Society, 2013, 96, 1085-1089.</fi<></scp>	_{12<}	/suþչ
52	Zn–Al Layered Double Hydroxide Film Functionalized by a Luminescent Octahedral Molybdenum Cluster: Ultraviolet–Visible Photoconductivity Response. ACS Applied Materials & Interfaces, 2020, 12, 40495-40509.	8.0	15
53	Robust, Transparent Hybrid Thin Films of Phase-Change Material Sb ₂ S ₃ Prepared by Electrophoretic Deposition. ACS Applied Energy Materials, 2021, 4, 9891-9901.	5.1	15
54	Fabrication of lead-free piezoelectric (Bi0.5Na0.5)TiO3–BaTiO3 ceramics using electrophoretic deposition. Journal of Materials Science, 2018, 53, 2396-2404.	3.7	14

#	Article	IF	CITATIONS
55	Electrophoretic deposition of Eu2+ doped CaALPHASiAlON phosphor particles for packaging of flat pseudo-white light emitting devices. Journal of the Ceramic Society of Japan, 2008, 116, 740-743.	1.1	13
56	Effect of bead-milling treatment on the dispersion of tetragonal zirconia nanopowder and improvements of two-step sintering. Journal of the Ceramic Society of Japan, 2009, 117, 470-474.	1.1	13
57	Fabrication of c-axis oriented zinc oxide by electrophoretic deposition in a rotating magnetic field. Journal of the European Ceramic Society, 2010, 30, 1171-1175.	5.7	13
58	Texture development in anatase and rutile prepared by slip casting in a strong magnetic field. Journal of the Ceramic Society of Japan, 2011, 119, 334-337.	1.1	13
59	Electrophoretic Coating of Octahedral Molybdenum Metal Clusters for UV/NIR Light Screening. Coatings, 2017, 7, 114.	2.6	13
60	Transparent functional nanocomposite films based on octahedral metal clusters: synthesis by electrophoretic deposition process and characterization. Royal Society Open Science, 2019, 6, 181647.	2.4	13
61	Fabrication of polystyrene colloidal crystal film by electrophoretic deposition. Advanced Powder Technology, 2020, 31, 3085-3092.	4.1	13
62	Development of novel boneâ€like nanocomposite coating of hydroxyapatite/collagen on titanium by modified electrophoretic deposition. Journal of Biomedical Materials Research - Part A, 2021, 109, 1905-1911.	4.0	13
63	Effect of Al2O3 addition on texturing in a rotating strong magnetic field and densification of B4C. Ceramics International, 2019, 45, 18222-18228.	4.8	12
64	Robust Structurally Colored Coatings Composed of Colloidal Arrays Prepared by the Cathodic Electrophoretic Deposition Method with Metal Cation Additives. ACS Applied Materials & Interfaces, 2020, 12, 40768-40777.	8.0	12
65	Textured Ti ₃ SiC ₂ by gelcasting in a strong magnetic field. Journal of the Ceramic Society of Japan, 2012, 120, 544-547.	1.1	11
66	Fabrication and Analysis of the Oriented <scp><scp>LiCoO</scp></scp> ₂ by Slip Casting in a Strong Magnetic Field. Journal of the American Ceramic Society, 2012, 95, 3428-3433.	3.8	11
67	Phosphor Deposits of β-Sialon:Eu2+ Mixed with SnO2 Nanoparticles Fabricated by the Electrophoretic Deposition (EPD) Process. Materials, 2014, 7, 3623-3633.	2.9	11
68	Beta-sialon phosphor deposits fabricated by electrophoretic deposition (EPD) process in a magnetic field. Ceramics International, 2014, 40, 8369-8375.	4.8	11
69	Original Synthesis of Molybdenum Nitrides Using Metal Cluster Compounds as Precursors: Applications in Heterogeneous Catalysis. Chemistry of Materials, 2020, 32, 6026-6034.	6.7	11
70	Revisiting properties of edge-bridged bromide tantalum clusters in the solid-state, in solution and vice versa: an intertwined experimental and modelling approach. Dalton Transactions, 2021, 50, 8002-8016.	3.3	11
71	Light-dependent ionic-electronic conduction in an amorphous octahedral molybdenum cluster thin film. NPG Asia Materials, 2022, 14, .	7.9	11
72	Pulsed-DC Electrophoretic Deposition (EPD) of Aqueous Alumina Suspension for Controlling Bubble Incorporation and Deposit Microstructure. Key Engineering Materials, 0, 412, 39-44.	0.4	10

#	Article	IF	CITATIONS
73	Colloidal processing of Li ₂ S–P ₂ S ₅ films fabricated via electrophoretic deposition methods and their characterization as a solid electrolyte for all solid state lithium ion batteries. Journal of the Ceramic Society of Japan, 2017, 125, 287-292.	1.1	10
74	Fabrication of BSCF-based mixed oxide ionic-electronic conducting multi-layered membrane by sequential electrophoretic deposition process. Journal of the European Ceramic Society, 2021, 41, 2709-2715.	5.7	10
75	Enhanced Piezoelectric Properties of Barium Titanate-Potassium Niobate Solid Solution System Ceramics by MPB Engineering. Key Engineering Materials, 2010, 445, 11-14.	0.4	9
76	Microstructure Control of Barium Titanate – Potassium Niobate Solid Solution System Ceramics by MPB Engineering and their Piezoelectric Properties. Key Engineering Materials, 2011, 485, 89-92.	0.4	9
77	Embedding hexanuclear tantalum bromide cluster {Ta6Br12} into SiO2 nanoparticles by reverse microemulsion method. Heliyon, 2018, 4, e00654.	3.2	9
78	Fabrication of BSCF-based mixed ionic-electronic conducting membrane by electrophoretic deposition for oxygen separation application. Journal of the European Ceramic Society, 2019, 39, 5292-5297.	5.7	9
79	Surface Modification on Cellulose Nanofibers by TiO2 Coating for Achieving High Capture Efficiency of Nanoparticles. Coatings, 2019, 9, 139.	2.6	9
80	Nest-like microstructured biocompatible membrane fabricated by hydrothermally-synthesized hydroxyapatite (HAp) whiskers. Journal of the European Ceramic Society, 2020, 40, 513-520.	5.7	9
81	Photoanode characteristics of dye-sensitized solar cell containing TiO2 layers with different crystalline orientations. Journal of Materials Research, 2009, 24, 1417-1421.	2.6	8
82	Positional-dependent luminescence property of β-SiAlON:Eu2+ phosphor particle. Applied Physics Letters, 2014, 104, .	3.3	8
83	Sinterable powder fabrication of lanthanum silicate oxyapatite based on solid-state reaction method. Journal of the Ceramic Society of Japan, 2015, 123, 274-279.	1.1	8
84	Fabrication of (111)-oriented Tetragonal BaTiO ₃ Ceramics by an Electrophoretic Deposition in a High Magnetic Field. Transactions of the Materials Research Society of Japan, 2015, 40, 223-226.	0.2	8
85	Observation of stacking faults and photoluminescence of laurate ion intercalated Zn/Al layered double hydroxide. Materials Letters, 2018, 213, 323-325.	2.6	8
86	ITO@SiO2 and ITO@{M6Br12}@SiO2 (M = Nb, Ta) Nanocomposite Films for Ultraviolet-Near Infrared Shielding. Nanoscale Advances, 0, , .	4.6	8
87	Optical and adhesive properties of composite silica-impregnated Ca-α-SiAlON:Eu2+ phosphor films prepared on silica glass substrates. Journal of the European Ceramic Society, 2012, 32, 1365-1369.	5.7	7
88	Fabrication of textured $\hat{l}\pm$ -alumina in high magnetic field via gelcasting with the use of glucose derivative. Journal of the Ceramic Society of Japan, 2013, 121, 89-94.	1.1	7
89	Effect of Electrode Reactions during Aqueous Electrophoretic Deposition on Bulk Suspension Properties and Deposition Quality. Key Engineering Materials, 2015, 654, 3-9.	0.4	7
90	Triaxial Crystalline Orientation of MgTi ₂ O ₅ Achieved Using a Strong Magnetic Field and Geometric Effect. Journal of the American Ceramic Society, 2016, 99, 1852-1854.	3.8	7

#	Article	IF	CITATIONS
91	Sintering and Ionic Conductivity of CuO-Doped Tetragonal ZrO2 Prepared by Novel Colloidal Processing Journal of the Ceramic Society of Japan, 2001, 109, 1004-1009.	1.3	6
92	Electrical Conductivity of a 3Y-TZP/Alumina Laminate Composite Synthesized by Electrophoretic Deposition Journal of the Ceramic Society of Japan, 2002, 110, 959-962.	1.3	6
93	Texturing Ca-ALPHASialon Via Strong Magnetic Field Alignment. Journal of the Ceramic Society of Japan, 2007, 115, 701-705.	1.1	6
94	Texturing of Si ₃ N ₄ Ceramics via Strong Magnetic Field Alignment. Key Engineering Materials, 2008, 368-372, 871-874.	0.4	6
95	Interaction between A-site deficient La0.8Sr0.2Ga0.8Mg0.2O3â^î^ (LSGM8282) and Ce0.9Gd0.1O3â^î^ (GDC) electrolytes. Solid State Ionics, 2014, 258, 18-23.	2.7	6
96	Effect of Surface Modification with TiO2 Coating on Improving Filtration Efficiency of Whisker-Hydroxyapatite (HAp) Membrane. Coatings, 2020, 10, 670.	2.6	6
97	Rapid Growth of Colloidal Crystal Films from the Concentrated Aqueous Ethanol Suspension. Langmuir, 2020, 36, 10683-10689.	3.5	6
98	Synthesis of Euâ€doped hydroxyapatite whiskers and fabrication of phosphor layer via electrophoretic deposition process. Journal of the American Ceramic Society, 2020, 103, 6780-6792.	3.8	6
99	Sequenced Successive Ionic Layer Adsorption and Reaction for Rational Design of Ni(OH)2/FeOOH Heterostructures with Tailored Catalytic Properties. ACS Applied Energy Materials, 2021, 4, 8252-8261.	5.1	6
100	Influence of niobium doping on phase composition and defect-mediated photoluminescence properties of Eu3+-doped TiO2 nanopowders synthesized in Ar/O2 thermal plasma. Journal of Alloys and Compounds, 2011, 509, 8944-8951.	5.5	5
101	Electrophoretic deposition of orientation-controlled zeolite L layer on porous ceramic substrate. Journal of the Ceramic Society of Japan, 2013, 121, 370-372.	1.1	5
102	Significantly improved photoluminescence of the greenâ€emitting βâ€sialon:Eu ²⁺ phosphor via surface coating of TiO ₂ . Journal of the American Ceramic Society, 2019, 102, 294-302.	3.8	5
103	Controllable Design of Various Microstructures for Hydroxyapatite Coatings by Electrophoresis Deposition Process for Biomedical Applications. Journal of the Electrochemical Society, 2019, 166, D700-D706.	2.9	5
104	Anisotropic Electric Conductivity and Battery Performance in <i>C</i> -axis Oriented Lanthanum Silicate Oxyapatite Prepared by Slip Casting in a Strong Magnetic Field. Materials Transactions, 2019, 60, 1949-1953.	1.2	5
105	Effect of crystalline orientation on photocatalytic performance for Nb-doped TiO2 nanoparticles. Advanced Powder Technology, 2021, 32, 4149-4154.	4.1	5
106	Two-step electrochemical deposition of Ni(OH)2/FeOOH bilayer electrocatalyst for oxygen evolution reaction. Materials Letters, 2022, 317, 132118.	2.6	5
107	Fabrication and characterization of zeolite bulk body containing mesopores and macropores using starch as pore-forming agent. Advanced Powder Technology, 2022, 33, 103626.	4.1	5
108	Texture development of surface-modified SiC prepared by EPD in a strong magnetic field. Journal of the Ceramic Society of Japan, 2011, 119, 667-671.	1.1	4

#	Article	IF	CITATIONS
109	Preparation and Characterization of Grain-Oriented Barium Titanate Ceramics Using Electrophoresis Deposition Method under a High Magnetic Field. Key Engineering Materials, 2011, 485, 313-316.	0.4	4
110	Magnesium ion distribution and defect concentrations of MgO-doped lanthanum silicate oxyapatite. Solid State Ionics, 2014, 258, 24-29.	2.7	4
111	Effect of ball-milling time and surfactant content for fabrication of 0.85(Bi _{0.5} Na _{0.5})TiO ₃ :0.15BaTiO <sub& green ceramics by electrophoretic deposition. Journal of the Ceramic Society of Japan, 2018, 126, 542-546.</sub& 	.gt:31.1	ub>
112	Effect of Aâ€site ion nonstoichiometry on the chemical stability and electric conductivity of strontium and magnesiumâ€doped lanthanum gallate. Journal of the American Ceramic Society, 2020, 103, 790-799.	3.8	4
113	Fabrication of textured B4C ceramics with oriented tubal pores by strong magnetic field-assisted colloidal processing. Journal of the European Ceramic Society, 2021, 41, 2366-2374.	5.7	4
114	Solutionâ€Based Approach for the Continuous Fabrication of Thin Lithiumâ€Ion Battery Electrodes by Wet Mechanochemical Synthesis and Electrophoretic Deposition. Advanced Engineering Materials, 2021, 23, 2100524.	3.5	4
115	Fabrication of Textured BaTiO ₃ Ceramics by Electrophoretic Deposition in A High Magnetic Field using Single-domain Particles. Transactions of the Materials Research Society of Japan, 2013, 38, 41-44.	0.2	4
116	Nanoarchitectonics of Glass Coatings for Near-Infrared Shielding: From Solid-State Cluster-Based Niobium Chlorides to the Shaping of Nanocomposite Films. ACS Applied Materials & Interfaces, 2022, 14, 21116-21130.	8.0	4
117	Hafnium Oxide Nanostructured Thin Films: Electrophoretic Deposition Process and DUV Photolithography Patterning. Nanomaterials, 2022, 12, 2334.	4.1	4
118	Aqueous Processing of Textured Silicon Nitride Ceramics by Slip Casting in a Strong Magnetic Field. Materials Science Forum, 2007, 534-536, 1009-1012.	0.3	3
119	Fabrication and Some Properties of Textured Ceramics by Colloidal Processing in High Magnetic Field. Key Engineering Materials, 2007, 352, 101-106.	0.4	3
120	Synthesis of Titania Thin Films by Cathodic Electrolytic Deposition. Journal of the Ceramic Society of Japan, 2007, 115, 818-820.	1.1	3
121	Surface Modification of SiC Powder for Use in Electrophoretic Deposition. Key Engineering Materials, 0, 412, 287-290.	0.4	3
122	Grain orientation of Nd-modified bismuth titanate ceramics by forming at low magnetic field. Journal of the Ceramic Society of Japan, 2014, 122, 58-62.	1.1	3
123	Influence of the crystal structure on the physical properties of monoclinic ZrO 2 nanocrystals. Nano Structures Nano Objects, 2015, 1, 1-6.	3.5	3
124	Magnetic properties of α″-Fe16N2-like compound derived from Fe3O4 fine powder coated on hard magnetic BaFe12O19 particles. Journal of Magnetism and Magnetic Materials, 2017, 443, 73-78.	2.3	3
125	Preparation of textured B ₄ C compact with oriented pore-forming agent by slip casting under strong magnetic field. Journal of the Ceramic Society of Japan, 2018, 126, 832-838.	1.1	3
126	Solution-mediated nanometric growth of α-Fe ₂ O ₃ with electrocatalytic activity for water oxidation. Nanoscale Advances, 2020, 2, 3933-3941.	4.6	3

#	Article	IF	CITATIONS
127	Production of crystal-oriented lanthanum silicate oxyapatite ceramics with anisotropic electrical conductivity and thermal expansion. Open Ceramics, 2021, 6, 100100.	2.0	3
128	Antibacterial-functionalized Ag loaded-hydroxyapatite (HAp) coatings fabricated by electrophoretic deposition (EPD) process. Materials Letters, 2021, 297, 129955.	2.6	3
129	Synthesis of novel hexamolybdenum cluster-functionalized copper hydroxide nanocomposites and its catalytic activity for organic molecule degradation. Science and Technology of Advanced Materials, 2021, 22, 758-771.	6.1	3
130	Material Texture and α-β Phase Transition of Self-assembled BaTiO ₃ /Polyvinylidene Fluoride Composites. Funtai Oyobi Fummatsu Yakin/Journal of the Japan Society of Powder and Powder Metallurgy, 2022, 69, 195-199.	0.2	3
131	Controlling the Deposition Process of Nanoarchitectonic Nanocomposites Based on {Nb6â^'xTaxXi12}n+ Octahedral Cluster-Based Building Blocks (Xi = Cl, Br; 0 ≤ ≤6, n = 2, 3, 4) for UV-NIR Blockers Coating Applications. Nanomaterials, 2022, 12, 2052.	4.1	3
132	Direct Shaping of Alumina Ceramics by Electrophoretic Deposition Using Conductive Polymer-Coated Ceramic Substrates. Advanced Materials Research, 2007, 29-30, 227-230.	0.3	2
133	Formation of Crystalline-Oriented Titania Thin Films on ITO Glass Electrodes by EPD in a Strong Magnetic Field. Key Engineering Materials, 2009, 412, 143-148.	0.4	2
134	Electrophretic Deposition of LDC/LSGM/LDC Tri-layers on NiO-YSZ for Anode-supported SOFC. Transactions of the Materials Research Society of Japan, 2010, 35, 723-725.	0.2	2
135	Textured Ti ₃ SiC ₂ by EPD in a Strong Magnetic Field. Key Engineering Materials, 0, 507, 15-19.	0.4	2
136	Crystalline-Oriented Beta-Sialon:Eu2+Deposits Fabricated by Electrophoretic Deposition (EPD) within Strong Magnetic Field. ECS Journal of Solid State Science and Technology, 2014, 3, R195-R199.	1.8	2
137	Rapid Fabrication of Colloidal Crystal Films by Electrophoretic Deposition and Its Application for a Volatile Liquid and Strain Detection Sensor. Journal of the Society of Powder Technology, Japan, 2019, 56, 339-346.	0.1	2
138	Shell-thickness control of hollow SiO2 nanoparticles through post-treatment using sol–gel technique toward efficient water confinement. Colloids and Surfaces A: Physicochemical and Engineering Aspects, 2021, 629, 127501.	4.7	2
139	Sedimentation classification treatment effect of starting powders in slip casting on magneto-orientation of mordenite zeolite. Transactions of the Materials Research Society of Japan, 2010, 35, 701-703.	0.2	2
140	Effect of CNT addition and its orientation on thermal shock resistance of B ₄ C/CNT composites fabricated by hot-pressing. Journal of Asian Ceramic Societies, 2022, 10, 370-377.	2.3	2
141	Orientation Control in Multilayered Alumina Prepared Using Electrophoretic Deposition in a Strong Magnetic Field. Advanced Materials Research, 2007, 29-30, 223-226.	0.3	1
142	Grain-Orientation Control of Bi ₅ FeTi ₃ O ₁₅ Ceramics Prepared by Magnetic-Field-Assisted Electrophoretic Deposition Method. Key Engineering Materials, 2008, 388, 205-208.	0.4	1
143	Control of Residual Stress in Multilayered Alumina Composites Prepared Using EPD in a Strong Magnetic Field. Key Engineering Materials, 0, 412, 233-236.	0.4	1
144	Preparation of Barium Titanate Grain-Oriented Ceramics and their Piezoelectric Properties. Key Engineering Materials, 0, 445, 3-6.	0.4	1

#	Article	IF	CITATIONS
145	Synthesis, Microstructure and Mechanical Properties of ZrB ₂ Ceramic Prepared by Mechanical Alloying and Spark Plasma Sintering. Key Engineering Materials, 2010, 434-435, 165-168.	0.4	1
146	Orientation Control of Hematite via Transformation of Textured Goethite Prepared by EPD in a Strong Magnetic Field. Key Engineering Materials, 2012, 507, 227-231.	0.4	1
147	The Characteristic of Inner Surface Coating on Porous Al ₂ O ₃ Tube by Electrophoretic Deposition. Key Engineering Materials, 2013, 545, 19-23.	0.4	1
148	Hydrothermal transformation of magnetically orientation-controlled seed layer into orientation-retained dense, continuous film in clear reaction solution. Journal of the Ceramic Society of Japan, 2013, 121, 550-554.	1.1	1
149	Fabrication of Textured Ceramics Using Mn and Nb-doped Hexagonal BaTiO ₃ by an Electrophoretic Deposition in a High Magnetic Field. Transactions of the Materials Research Society of Japan, 2014, 39, 199-202.	0.2	1
150	Video Processing Electrophoretic Measurements under High Electric Fields for Sub-millimeter Particles in Oil. Journal of Oleo Science, 2022, 71, 445-457.	1.4	1
151	Sintering Characteristics of Iron Ultrafine Powders. Solid State Phenomena, 1992, 25-26, 179-186.	0.3	0
152	Design of Alumina/Alumina Laminate Composites with Crystalline-Orientated Layers Produced by Electrophoretic Deposition under a High Magnetic Field. Key Engineering Materials, 2006, 314, 25-32.	0.4	0
153	Mechanical Properties of Textured Alumina Prepared by Colloidal Processing in a Strong Magnetic Field. Materials Research Society Symposia Proceedings, 2006, 977, 1.	0.1	0
154	Thermoelectric Properties and Magnetic Anisotropies of Magnetically Grain-Oriented Sr- or Bi-doped Ca3Co4O9 Thick Films. Materials Research Society Symposia Proceedings, 2007, 1044, 1.	0.1	0
155	Improvement of Thermoelectric Properties of p- and n-types Oxide Thick Films Fabricated by Electrophoretic Deposition. Materials Research Society Symposia Proceedings, 2007, 1044, 1.	0.1	0
156	Hydrogen Storage Properties of Nb-Zr-Fe Alloys Disintegrated by Hydrogen Gas. Materials Science Forum, 2007, 534-536, 73-76.	0.3	0
157	Fabrication of Highly Microstructure Controlled Ceramics by Novel Colloidal Processing. Key Engineering Materials, 0, 336-338, 2372-2377.	0.4	0
158	Textured PbTiO ₃ Based Ceramics Fabricated by Slip Casting in a High Magnetic Field. Key Engineering Materials, 0, 421-422, 395-398.	0.4	0
159	Fabrication of Multi-Layered Thermoelectric Thick Films and their Thermoelectric Performance. Key Engineering Materials, 2009, 412, 291-296.	0.4	0
160	UV Protection Mechanism and Property of Functional Ceramic Particles. Hyomen Kagaku, 2014, 35, 45-49.	0.0	0
161	Textured Beta-Sialon:Eu ²⁺ Phosphor Deposits Fabricated by Electrophoretic Deposition (EPD) Process within a Strong Magnetic Field: Preparation Process and Photoluminescence (PL) Properties Depending on Orientation. Key Engineering Materials, 0, 654, 268-273.	0.4	0
162	Surface Modification of Complex Oxide Powder with Polyelectrolyte Layers Improving EPD Characteristics. Key Engineering Materials, 0, 654, 255-260.	0.4	0

#	Article	IF	CITATIONS
163	Fabrication of c-Axis-Oriented Zeolite L Seed Layer on Porous Zirconia Substrate by Electrophoretic Deposition in Strong Magnetic Field. Key Engineering Materials, 0, 654, 274-279.	0.4	0
164	Anisotropic Electronic Conductivity and Battery Performance in C-axis Oriented Lanthanum Silicate Oxyapatite Prepared by Slip Casting in a Strong Magnetic Field. Funtai Oyobi Fummatsu Yakin/Journal of the Japan Society of Powder and Powder Metallurgy, 2018, 65, 121-126.	0.2	0
165	Microstructure Control of Ceramic Functional Membrane by Electrophoretic Deposition Method and Its Application to Oxygen Separation Membrane using Mixed Ionic-Electronic Conductor. Funtai Oyobi Fummatsu Yakin/Journal of the Japan Society of Powder and Powder Metallurgy, 2021, 68, 121-128.	0.2	0
166	Fabrication of YSZ-Carbon Felt Composite Materials by Spark Plasma Sintering Process. Key Engineering Materials, 0, 904, 339-343.	0.4	0